Formulation, Development, and Evaluation of Bosentan Monohydrate Spray Dried- Solid Dispersion Tablets for Improved Dissolution Profile

Sayali Raut[1], Ashok Hajare[2*], Rutuja Chougale[3], Shubham Kamble[1], Kiran Patil [3]

[1]Department of Pharmaceutics, Bharati Vidyapeeth College of Pharmacy, Near Chitranagari, Kolhapur, Maharashtra, India.
[2]Department of Pharmaceutical Technology, Bharati Vidyapeeth College of Pharmacy, Near Chitranagari, Kolhapur, Maharashtra, India.
[3]Department of Pharmaceutical Quality Assurance, Tatyasaheb Kore College of Pharmacy, Warananagar, Maharashtra, India.

ABSTRACT

Bosentan monohydrate (BM) is utilized for the treatment of pulmonary arterial hypertension, exhibiting poor aqueous solubility and bioavailability. This study aims to enhance the dissolution rate of the drug using Eudragit®EPO through spray drying. The drug and Eudragit®EPO were combined in ratios of 1:1, 1:2, 1:3, 1:4, and 1:5 (w/w) to generate compositions SD1 to SD5. SD5, at a 1:5 drug-to-carrier ratio, demonstrated a statistically significant increase in saturation solubility and drug content. Six tablet formulations (F1 to F6) containing SD5 and tableting excipients were developed and processed. Formulation F2, consisting of 26.36% HPMC K4M and 23.63% MCC, exhibited the highest dissolution and drug release. The probable mechanism underlying BM dissolution in SD involves its amorphous form and the solubilizing effect facilitated by hydrogen bonding between BM and Eudragit®EPO. The carrier's binding effect likely contributed to high tensile strength, low friability, and extended disintegration time. Direct mixing of SD with HPMC might have improved the uniformity of SD within the tablet matrix and the release profile. This study demonstrates the efficacy of spray drying in preparing SD of BM with Eudragit®EPO, potentially enhancing its solubility and stability.

Keywords: Bosentan monohydrate, Eudragit®EPO, Solubility, Dissolution, Solid-dispersion, Spray drying.

1. INTRODUCTION

It is commonly recognized that approximately 40% of recently developed medications exhibit low water solubility, compromising absorption and increasing gastro mucosal toxicity. Three primary criteria affecting a drug's bioavailability include its solubility, permeability, and dissolution [1]. According to the Biopharmaceutical Classification System (BCS), drugs are categorized based on their solubility and permeability [2]. Drugs with poor solubility belong to BCS class II and IV. The poor solubility of drugs poses a challenge to bioavailability. In such cases, strategies such as particle size reduction, polymorphism, molecular encapsulation, incorporation of surface-active agents, and solid dispersion (SD) can be employed to enhance solubility [3]. In the case of SD, the carrier component dissolves upon exposure to aqueous solutions, releasing drug molecules as tiny, dispersed particles [4]. The bioavailability of weakly water-soluble drugs is ultimately improved due to increased surface area and dissolution rate. By reducing particle size and increasing particle porosity, the drug in a soluble hydrophilic carrier enhances the rate of dissolution [5]. Therefore, enhancing the bioavailability of these medications and minimizing their negative effects by altering their drug release profile is conceivable.

SD is a prominent technique used for dissolution rate and solubility enhancement, as well as for improving the oral absorption of weakly water-soluble drugs [2]. SD is a composite mixture prepared by mixing one or more solid

Corresponding author: Ashok A. Hajare
ashok.hajare@bharatividyapeeth.edu
Received: 6/10/2022 Accepted: 25/6/2023.
DOI: https://doi.org/10.35516/jjps.v16i4.514

particles and dispersing them into an inert medium through fusion, solvent evaporation, or the melting method. SD contains a hydrophilic matrix for solubility enhancement and a hydrophobic drug whose solubility is to be improved, wherein the matrix can be either crystalline or amorphous [6]. SD was originally used to create a eutectic combination of pharmaceuticals with water-soluble carriers to overcome the limited bioavailability of lipophilic drugs [7,8]. Spray drying is a superior method compared to other methods as it operates at comparatively low temperatures, preventing most decomposition that occurs during the fusion process in the melting method. Spray drying has no solvent limitations and is most suitable for large-scale production [9]. Previously, SD of BM was made using hydroxypropyl β-cyclodextrin (HP β-CD) and polyethylene glycol (PEG) 4000 polymers, but BM in such SD retained its crystallinity, limiting its solubility [10]. Additionally, PEG 4000 exhibits an uncontrolled rate of hydration, rheological changes during shelf-life, and the possibility of microbial contamination during use [6].

Eudragit® EPO is a cationic polyelectrolyte belonging to methacrylate copolymers. It is composed of dimethylaminoethyl methacrylate, butyl methacrylate, and methyl methacrylate in a molar ratio of 2:1:1 [11]. It carries a positive charge, so when dissolved in an aqueous medium, it forms a solid dispersion (SD) with a drug that has a negative charge [12]. Samples containing coated drug particles, as well as reference formulations with an equivalent amount of this polymer, exhibited higher tensile strength, lower friability, and longer disintegration times [11]. These outcomes result from the binding effect exhibited by Eudragit® EPO. Additionally, a modified processing method, in which the molten drug-carrier mass was directly mixed with hydroxypropyl methylcellulose (HPMC), improved the uniformity of the drug in the tablet matrix and the release profile [13].

Bosentan monohydrate (BM) is used to treat pulmonary artery hypertension (PAH) and possesses dual endothelin receptor antagonistic characteristics [14]. The structure of BM is shown in Figure 1.

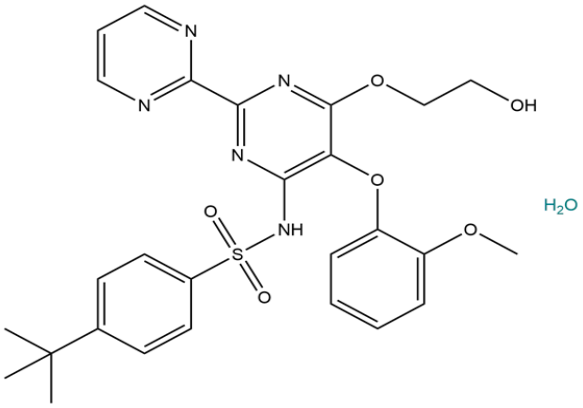

Figure 1. Structure of Bosentan Monohydrate

BM is prescribed at a daily dose of 125–250 mg for treating pulmonary arterial hypertension (PAH). It exhibits a plasma peak concentration between 3-5 hrs after administration, with a biological half-life of 5.4 hrs [15]. The oral bioavailability of BM is 50%, with variability in its absorption due to its poor aqueous solubility. The aqueous solubility of BM is 1 mg/100 mL, categorizing it as BCS class II [16]. Hence, the present study aimed to formulate BM-loaded Eudragit® EPO solid dispersion (SD) microparticles with the primary objective of

achieving rapid drug release in the acidic pH of the stomach. To enhance solubility, SD was attempted by spray drying using polymers along with hydroxypropyl β-cyclodextrin (HP β-CD). Additionally, efforts were made to formulate tablets of SD with hydroxypropyl methylcellulose (HPMC) K4M, microcrystalline cellulose (MCC) as binders, and talc and magnesium stearate as glidant and lubricant to create an improved dissolution profile for therapeutic effectiveness.

2. RESULTS AND DISCUSSION

Particles produced through spray drying have smaller sizes, enhancing their surface area and expediting the dissolution process.

The carrier incorporated in the solid dispersion (SD) significantly improves the drug's solubility through enhanced particle wettability, thereby increasing the drug's bioavailability. Drugs formulated as SD exist as supersaturated solutions in metastable polymorphic forms, leading to increased solubility and availability in the amorphous state [17, 18, 19]. Therefore, SD of the poorly soluble Bosentan monohydrate (BM) was formulated to enhance its solubility.

The well-known gastro-soluble polymer Eudragit® E100 is available in powder form as Eudragit® EPO. Tertiary amino groups in the polymer ionize at an acidic pH, making Eudragit® E100 soluble in gastric fluid when the pH is lower than 5. Researchers have utilized Eudragit® E100 to prepare SD of hydrophobic drugs with dissolution rate-dependent bioavailability due to its excellent solubility in gastric fluids [20].

2.1 Preparation and optimization of SD

Improved bioavailability results from the increased surface area achieved through small particle size. Spray drying was employed to produce SD, as it allows for rapid solvent evaporation, quickly converting the drug-carrier solutions into solid particles. The prepared SD was further evaluated for the following parameters.

2.2 Evaluation of SD powder:

SD compositions (SD1 to SD5) were optimized by evaluating the prepared SD for drug content and saturation solubility.

2.2.1 Flow properties and Heckel plot of SD powder:

The solid dispersion (SD) compositions were evaluated for various flow properties, including the angle of repose, Hausner's ratio, and Carr's index. The results are displayed in the table below. The SD5 composition exhibits an angle of repose of 27.32±0.2°, Hausner's ratio of 1.18±0.85, and Carr's index of 14.7±0.47%, indicating good flow and compressibility for the SD5 composition [21].

Table 1. Flow properties of BM SD

Batch code	Angle of Repose (°)	Bulk density (g/cm^3)	Tap density (g/cm^3)	Hausner's ratio	Carr's index (%)
SD1	42.40±0.3	0.4718±0.019	0.6178±0.021	1.31±0.16	23.6±0.41
SD2	46.10±0.6	0.4627±0.017	0.5547±0.042	1.20±0.21	16.6±0.11
SD3	38.20±0.5	0.4579±0.036	0.5741±0.063	1.25±0.42	20.2±0.17
SD4	48.19±0.9	0.4905±0.085	0.5853±0.051	1.19±0.57	16.2±0.58
SD5	27.32±0.2	0.4375±0.074	0.5131±0.011	1.18±0.85	14.7±0.47

(n= 3, mean±SD)

The Heckel plot for the BM-loaded Eudragit® EPO solid dispersion (SD) exhibited a Type C curve, indicating particle rearrangement and fragmentation of large aggregates under low compressional pressure. As the compression force increased, the curves became linear due to plastic deformation. It can be inferred that the curved

region at low pressures is associated with individual particle movement in the absence of interparticle bonding. The transition from curved to linear corresponds to the minimum pressure required to form a coherent compact, indicating the formation of coherent compacts in this region.

Table 2. Heckel plot of BM SD

Pressure (Tons)	Thickness (cm)	Diameter (cm)	Radius (cm)	Weight of tablet (mg)	Volume (πr^2h)	Density (mg/ml)	Hardness (Kg/cm^2)	Relative density	1/1-RD	In (1/1-RD)
0.5	0.31±0.3	0.8	0.4	200±0.1	0.1557±0.4	1284.52±0.7	4±0.1	0.7739	4.42	1.4861
1	0.30±0.1	0.8	0.4	200±0.7	0.1507±0.2	1327.14±0.1	5±0.3	0.7996	4.99	1.6074
1.5	0.29±0.2	0.8	0.4	200±0.5	0.1456±0.1	1373.62±0.2	7±0.2	0.8276	5.80	1.7578
2	0.27±0.5	0.8	0.4	200±0.4	0.1356±0.3	1474.92±0.1	8±0.4	0.8886	8.97	2.1938
2.5	0.24±0.4	0.8	0.4	200±0.6	0.1205±0.6	1659.75±0.5	9±0.5	1	-	
3	0.24±0.6	0.8	0.4	200±0.2	0.1205±0.5	1659.75±0.4	9±0.1	1	-	

(n= 3, mean±SD)

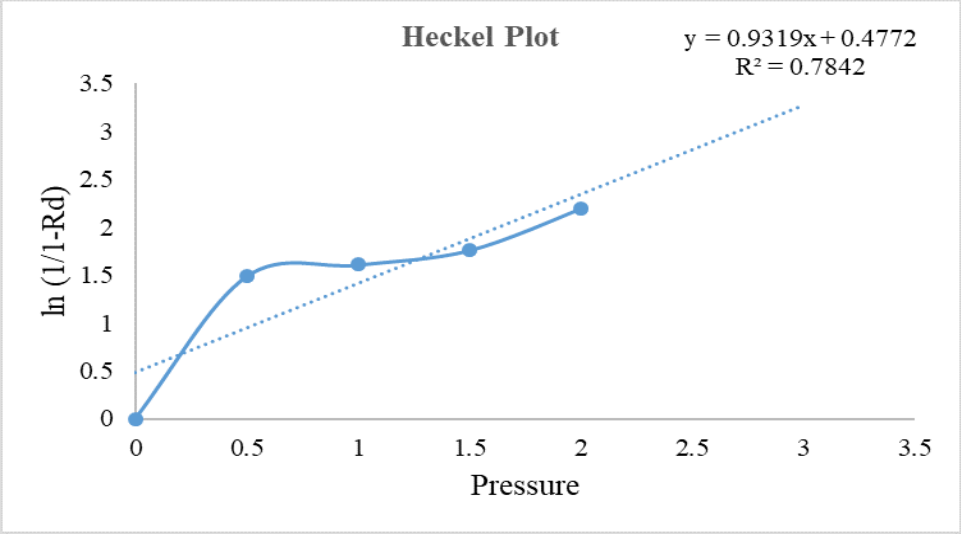

Figure 2. Heckel plot of BM-loaded Eudragit® EPO SD

2.2.2 Scanning Electron Microscopy (SEM):

SEM studies were conducted to qualitatively examine the shape and surface morphology of the BM-loaded Eudragit® EPO solid dispersion (SD), and the obtained images are presented in Figure 3. According to Lee H et al., the pure bosentan drug exhibited irregular, non-spherical morphology, a polydisperse size range, and a crystalline particle state. In contrast, the BM-loaded Eudragit® EPO SD revealed irregularly folded and flocculated round morphology with a smooth surface and monodisperse size range.

The differences in particle morphology between the pure drug and the spray-dried formulations suggested the conversion of the drug from a crystalline form to an amorphous form, consistent with the XRPD results [22].

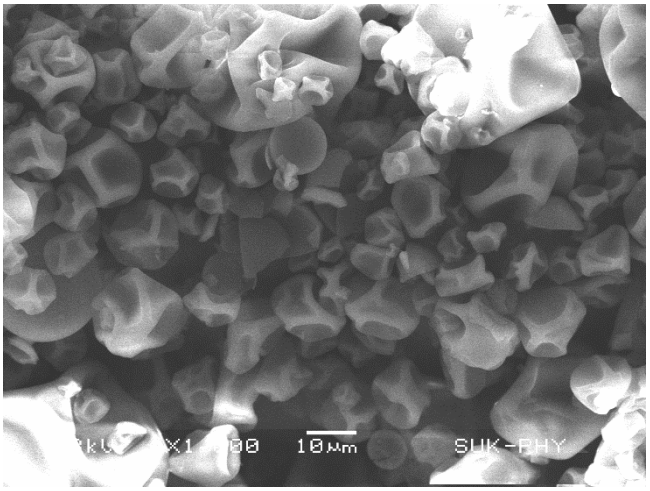

Figure 3. SEM of BM-loaded Eudragit® EPO SD

2.2.3 Particle size:

The particle size of the spray-dried dispersions is presented in Table 3. The SD5 composition has the smallest particle size of 213.4 nm, which enhances the surface area of smaller particles, promoting better wetting and faster dissolution. This, in turn, leads to improved drug solubility and bioavailability. Consequently, SD5 will be utilized for further formulation [22].

Table 3. Particle size of BM SD5

Batch code	Particle Size (nm)
SD5	213.4±0.6

(n= 3, mean±SD)

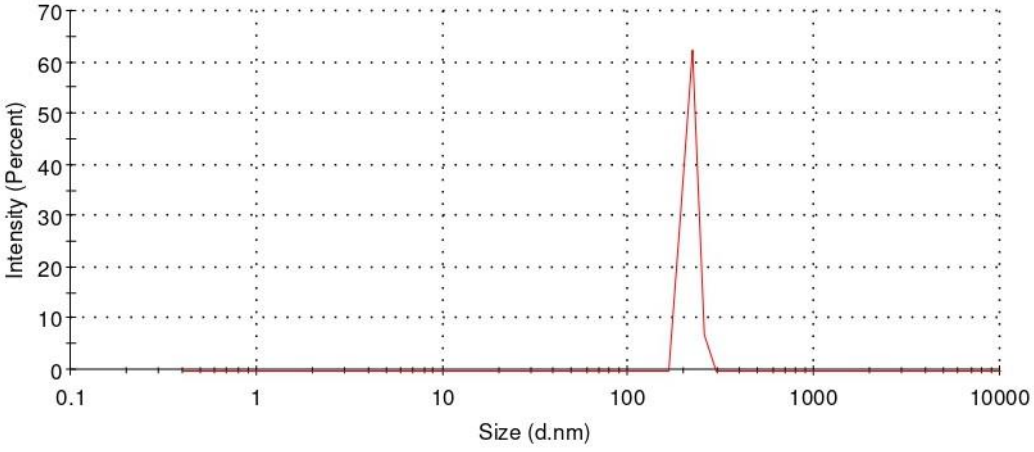

Figure 4. Particle size of BM-loaded Eudragit® EPO SD5

2.2.4 Drug content:

The spray-dried dispersions were solid, free-flowing, fine powder with a drug content of 74.2% and 94.4%, as shown in Table 4. SD5 exhibited a drug content of 94.4 ± 0.9% with uniform drug distribution, good flowability, and compressibility, as observed in the flow properties.

2.2.4 Saturation solubility:

Saturation solubility showed statistically significant improvements in solubility, increasing from 55.54±0.21 to 138.16±0.47 µg/mL. BM was formulated into SD employing a carrier Eudragit® EPO at a 1:5 ratio, as detailed in Table 4. In SD, the saturation solubility of BM increased to 138.16±0.47 µg/mL. Based on the overall evaluation, especially the saturation solubility and drug content, the composition SD5 was selected for preparing tablet formulations.

Table 4. Drug content and saturation solubility of BM SD

Batch code	BM : Eudragit® EPO ratio	Solubility in water (mg/mL)	Drug content (%)	Saturation solubility (mg/mL)
Pure drug	-	0.009	-	50.61±.043
SD1	1:1	0.085	74.2±0.5	55.54±.021
SD2	1:2	0.091	82.7±0.7	88.72±0.19
SD3	1:3	0.098	83.9±0.4	104.33±0.36
SD4	1:4	0.099	91.5±0.1	123.63±.058
SD5	1:5	0.103	94.4±0.9	138.16±0.47

(n= 3, mean±SD)

2.3 Formulation of tablets:

The composition SD5 was selected for the formulation of tablets among various compositions. The wet granulation technique was employed in this instance for tablet creation. HPMC K4M and MCC were used as binders, while talc and magnesium stearate served as glidant and lubricant. The choice of HPMC K4M was based on its ease of usage, better compressibility, high drug loading capacity, good stability over a wide pH range, and quick swelling [23]. MCC was selected for its ability to hold water, aiding in uniform granulation [24]. Talc was included to reduce interparticulate friction, van der Waals forces, and electrostatic charges, improving powder flow properties [25]. Magnesium stearate, an affordable and chemically stable lubricant, was used for its high lubrication power and high melting point [26]. Six tablet formulations, F1 to F6, were designed using SD5 and other tableting excipients, as detailed in Table 5.

Table 5. The formulation composition of BM SD tablets

Compoenents (mg)	F1	F2	F3	F4	F5	F6
SD5 powder	90	90	90	90	90	90
HPMC K4M	56.74	52.73	48.75	44.74	40.73	37.75
MCC	43.26	47.27	51.25	55.26	59.27	62.25
Talc	7	7	7	7	7	7
Magnesium stearate	3	3	3	3	3	3
Total weight	200.0	200.0	200.0	200.0	200.0	200.0

2.4 Evaluation of Tablets:

Six tablet formulations (F1-F6) were prepared and evaluated to determine an optimized tablet formulation.

2.4.1 Thickness:

Tablet thickness is crucial for administration comfort and therapeutic efficacy [27]. It influences disintegration and dissolution behavior. The thickness of tablet formulations (F1-F6), measured by digital vernier caliper, ranged from 2.85±0.42 to 3.92±0.05 mm, as shown in Table 6. This falls within the pharmacopoeial limit for thickness, which specifies that the tablet diameter should be 8 mm or less.

2.4.2 Hardness:

Tablet hardness should be within an optimal range, as both excessively high and low hardness can impact disintegration. The hardness of the tablets was determined using the Monsanto hardness tester. The hardness of all tablet formulations was in the range of 3.7±0.47 to 5±0.31 kg/cm2, as detailed in Table 6. This falls within the pharmacopoeial specifications of 3-6 kg/cm^2.

2.4.3 Friability:

Tablet friability measures the resistance of compressed tablets against coating and packaging during manufacturing and shipping. The pharmacopoeial limit for friability is less than 1% of the tablet mass. The % loss of tablets for formulations F1-F6 ranged from 0.38±0.02 to 0.54±0.03%, as indicated in Table 6. The friability test results suggest compliance with the official limits, ensuring sufficient tablet strength.

2.4.4 Weight variation:

Tablet weight variation is crucial for verifying dosage consistency and supporting tablet strength, safety, and identity. The weight variation of tablets in each batch was assessed using an analytical balance, as detailed in Table 6. The % weight variation for batches F1-F6 ranged from 4.18±0.07 to 7.54±0.8%, in compliance with pharmacopoeial specifications of ±7.5%.

2.4.5 Disintegration time:

Disintegration time reflects the duration needed to break down a tablet into smaller pieces, creating a larger surface area for faster dissolution. In vitro disintegration time was determined using a disintegration tester, and the results for formulations F1 through F6 ranged from 32±5 to 45±1 sec, as presented in Table 6. These values align with pharmacopoeial standards of 3 minutes.

2.4.6 Drug content:

The drug content of all prepared tablet formulations was assessed using a UV-visible spectrophotometer. The drug content in formulations ranged from 93.15±0.2 to 95.41±0.05%, as shown in Table 6. Formulation F2 exhibited the highest drug content at 95.41±0.05%, surpassing the values obtained for other formulations.

Table 6. Evaluation of bosentan tablets

Batch code	Thickness (mm)	Hardness (kg/cm^2)	Friability (%)	Weight variation (%)	Disintegration time (sec)	Drug content (%)
F1	2.91±0.21	4.5±0.23	0.39±0.05	4.56±0.10	36±2	93.55±0.21
F2	3.92±0.05	5.0±0.31	0.54±0.03	7.54±0.8	45±1	95.41±0.05
F3	2.85±0.42	4.4±0.73	0.38±0.02	5.22±0.12	38±3	94.85±0.75
F4	3.75±0.81	4.5±0.99	0.45±0.08	4.18±0.07	40±4	93.15±0.12
F5	2.94±0.58	3.9±0.93	0.39±0.09	3.17±0.5	33±6	94.32±0.32
F6	2.86±0.65	3.7±0.47	0.45±0.04	2.45±0.20	32±5	94.62±0.89

(n= 3, mean±SD)

Based on the data analysis of the evaluated tablet characteristics, including a thickness of 3.92±0.05 mm, hardness of 5.0±0.31 kg/cm2, friability of 0.54±0.03%, weight variation of 7.54±0.8%, disintegration time of 45±1 sec, and drug content of 95.41±0.05%, Formulation F2 was concluded to be the optimized one.

2.4.7 *In vitro* drug release:

In vitro drug release from plain BM and the optimized F2 BM SD was studied using USP XXII type II dissolution test equipment. The results of in vitro drug release were plotted as cumulative percent drug release vs. time, as illustrated in Fig. 1. At the end of 9 hours, Formulation F2 exhibited the highest dissolution rate of 98.21%, while for the same duration, the release from plain BM was 38.7%. Comparisons with previously reported work concluded that BM could be successfully formulated with HPMC K4M and HPMC K15M. Formulation containing BM: HPMC K4M in the ratio 1:0.5 was optimized, maintaining a drug release of 96.3 ± 0.53% for 12 hours. Furthermore, the cumulative drug release obtained through the dissolution study of BM formulated with Eudragit® EPO was 98.21%, sustaining drug release up to 9 hours. Therefore, the BM tablet formulation containing Eudragit® EPO appeared as an effective polymer that enhanced the drug's dissolution ability.

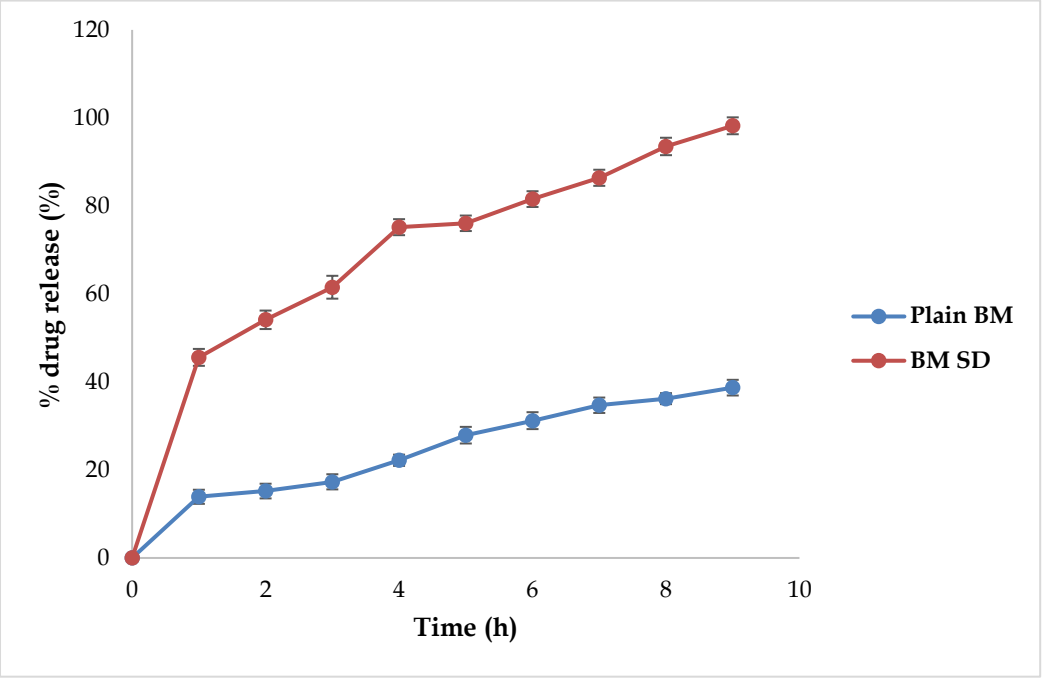

Figure 5.A plot of Cumulative % Drug Release versus Time of Plain BM and BM SD

2.4.8 XRPD Analysis:

The X-ray powder diffraction pattern of pure BM and Formulation F2 is presented in Fig. 2. The drug's diffractogram pattern was indicated by the existence of sharp peaks at 21.8º and 27.8º, confirming its crystallinity. In Formulation F2, in addition to a decrease in the sharpness of peaks, the multiple sharp peaks that were present with the plain drug were statistically decreased, suggesting amorphization of the drug. This physical change demonstrates that the BM was dissolved to a molecular level in a SD, which further controls the drug's ability to effectively dissolve in the medium [28].

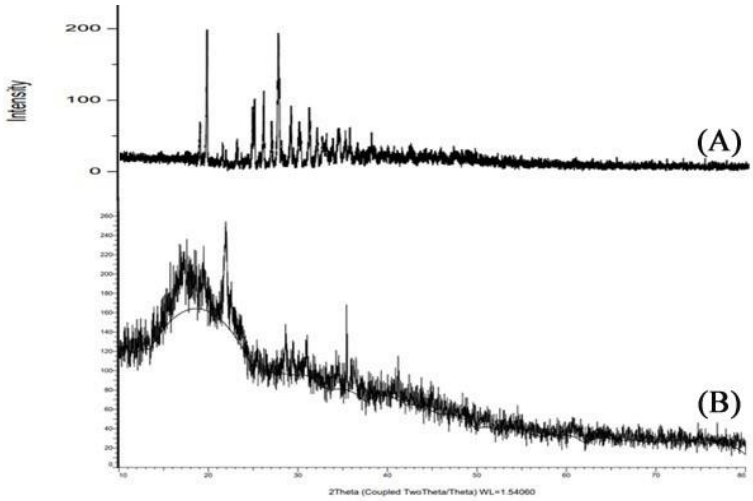

Figure 6. XRPD Analysis of (A) Bosentan monohydrate and (B) F2 formulation

2.4.9 FTIR Analysis:

The FTIR distinctive peaks in BM, Fig. 3, appeared at 2960.73 cm^{-1} for CH_3-stretching, 3493.09 cm^{-1} for OH-stretching, 1080.14 cm^{-1} for C-O stretching in ether, and 1384.89 cm^{-1} for S=O stretching. The CH_3 and OH stretching peaks at 2927 cm^{-1} and 3383 cm^{-1} for formulation F2 showed only a minor change. It reflects intermolecular hydrogen bonding potential of F2 formulation. These findings were close to results reported by Hajare et al. (2020) for clobetasol propionate [29].

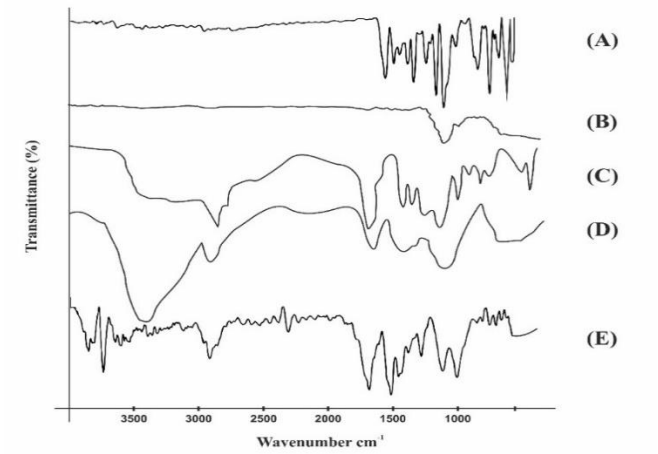

Figure 7. FTIR spectra of (A) Bosentan monohydrate and (B) HPMC K4M (C) Eudragit EPO (D) MCC (E) F2 formulation

2.4.10 DSC Analysis:

A popular thermal analysis method known as differential scanning calorimetry (DSC) provides accurate data on a material's physical and energetic properties. The melting point endotherm of BM was found to be at 104.2 ℃, whereas that of the F2 batch was found at 68.8 ℃. The DSC thermogram of formulation F2 showed reduced and diffused endothermic peaks, as seen in Figure 7. The

diffused DSC pattern of the formulation indicated that the endothermic peak had shifted, and its strength had decreased, indicating that the drug had changed from being crystalline. The drug's dissolving rate statistically increased as a result of its conversion from the crystalline to the amorphous state, as the latter has high internal energy and is thought to be in a highly disordered condition [30].

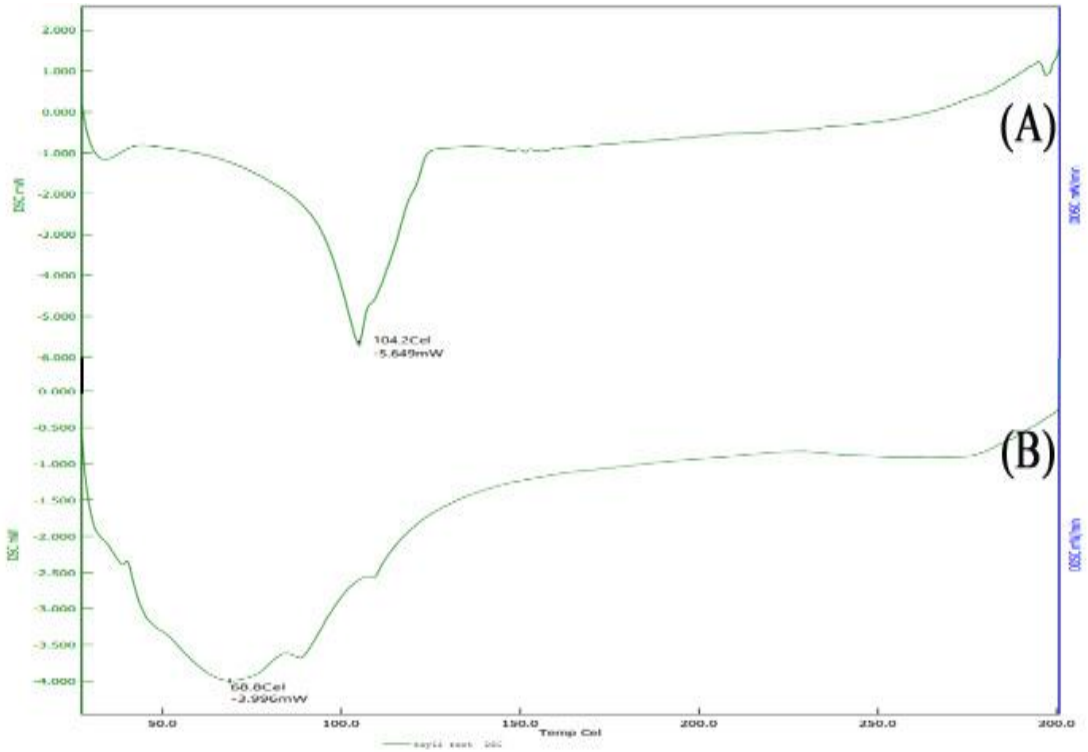

Figure 8. DSC Thermogram of (A) Bosentan monohydrate and (B) F2 formulation

2.4.11 Drug release kinetics study:

To estimate the mechanism of drug release from SD, the in vitro release data was fitted to multiple drug release kinetics models. The findings showed that the formulation was best explained by Higuchi release kinetics (square root kinetics), as depicted in Figure 6, indicating that the drug diffuses at a slower pace as the distance for diffusion increases.

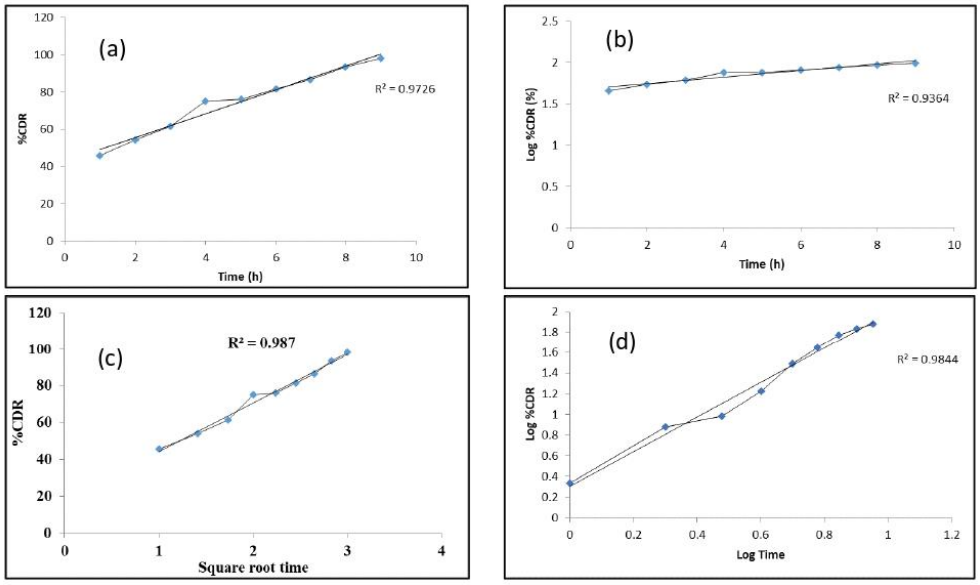

Figure 9. Comparative plots of (a) zero-order release kinetics, (b) first-order release kinetics, (c) Higuchi (SQRT) release kinetics, and (d) Korsemeyer-Peppas model for the selected SD formulation

2.4.12 Stability study:

According to ICH guideline requirements, stability tests of the optimized formulation F2 were performed for three months at 40°C and a relative humidity of 75%. After 90 days, the sample was removed and tested for drug content and percent drug release, as shown in Table 7. At the end of the 3 months, the drug content was within the pharmacopoeial limit (95.32%), indicating that the prepared solid dispersion of BM was stable.

Table 7. Drug content and release data for stability study

Sr. No.	Drug content (%)		Drug release (%)	
	0^{th} Day	90^{th} Day	0^{th} Day	90^{th} Day
1	95.41	95.35	98.21	98.12
2	95.48	95.21	98.30	98.21
3	95.35	95.40	98.28	98.31
Mean	95.41±0.053	95.32±0.080	98.26±0.038	98.21±0.077

(n= 3, mean±SD)

3. CONCLUSION

BM, classified as a BCS Class II drug, poses challenges due to its poor water solubility. Eudragit® EPO, a newly introduced polymer, has been investigated for its ability to enhance solubility and dissolution of BM. The preparation of solid dispersion complexes of the drug with Eudragit® EPO using spray drying has proven effective in enhancing the drug's solubility and dissolution. The likely mechanism behind the improved dissolution of BM involves a physical change in the state of the solid dispersion and the solubilizing effects facilitated by hydrogen bonding formed between Eudragit® EPO and the drug molecules.

Further exploration of Eudragit® EPO in extensive research, encompassing various model drugs, stability studies, and clinical testing, is warranted.

4. MATERIALS AND METHODS

4.1 Materials

Bosentan monohydrate was provided by Megafine Chemicals Pvt. Ltd., Mumbai, India. Evonik Industries Pvt. Ltd., Mumbai, supplied Eudragit® EPO. HPMC K4M was purchased from Loba Chem Ltd., Mumbai, India. Analytical-grade chemicals were utilized for all compounds and reagents.

4.2 Preparation and optimization of solid dispersion:

Solid dispersion (SD) was created via spray drying because it enables speedy solvent evaporation, resulting in a quick transformation of the drug: carrier solution into solid particles. Different drug carrier ratios of BM were dissolved in methanol (10% w/v) with Eudragit® EPO (1:1, 1:2, 1:3, 1:4, and 1:5). To obtain a clear solution, the liquids were thoroughly mixed. Using a spray drier (Labultima, Mumbai, India), the clear solutions were dried at an inlet temperature of 80 °C, output temperature of 55 °C, feed pump rate of 8 mL/min, aspiration rate of 45 mbar, and atomization air pressure of 2.5 kg/cm2. To remove any remaining solvents, the resultant SD was vacuum desiccated for 24 h. The dried bulk was then triturated and passed through mesh 80 to ensure a consistent particle size and kept in a tightly sealed container until it was used [31]. Furthermore, the prepared compositions were evaluated for drug content and saturation solubility to optimize the composition of BM SD.

4.3 Evaluation of prepared solid dispersion:

4.3.1 Flow properties and Heckel plot of SD powder:

A. Angle of repose

The angle of repose is a measurement of a powder's or granules' flowability. The powder is carried freely through the fixed funnel to create a heap of specified height, and the angle formed by the powder with that of the base is determined, from which the flow type of the sample is identified. The powder's angle of repose was calculated using the fixed funnel free-standing cone technique using the formula [21]:

$$\theta = \tan^{-1}\frac{h}{r} \quad \text{……. (Equation 1)}$$

Where, h: Height between the lower tip of a funnel and the base of a heap of granules, r is the radius of the base of heap formed.

B. Bulk density

The bulk density of all batches of S-SNEDDS was assessed by gently pouring 5g of powder through a glass funnel into a 10 mL graduated cylinder and recording the volume filled by the sample. The following formula was used to compute the bulk density [21]:

$$\text{Bulk density}\left(\frac{g}{mL}\right) = \frac{\text{Weight of samples in g}}{\text{Volume occupied by sample}} \quad \text{(Equation 2)}$$

C. Tapped density

A glass funnel was used to pour 5 g of powder into the 10 mL graduated cylinder. A consistent volume was attained by tapping the cylinder from a distance of 2 inches. After recording the volume of powder occupied after tapping, the tapped density was obtained as follows [21]:

$$\text{Tapped density}\left(\frac{g}{mL}\right) = \frac{\text{Weight of samples (g)}}{\text{Tapped volume occupied by sample}} \quad \text{(Equation 3)}$$

D. Hausner's ratio

The Hausner ratio was calculated to characterize the flow of a powder blend. When the Hausner ratio exceeds 1.25, it is regarded to be a sign of poor flowability. The following was the formula [21]:

$$\text{Hausner's ratio} = \frac{\text{Tapped bulk density}}{\text{Loose bulk density}} \quad \text{(Equation 4)}$$

E. Carr's Compressibility Index (CCI)

Carr's compressibility index was calculated with the

formula as follows [21]:

$$\%CCI = \frac{TBD-LBD}{TBD} x\ 100 \ldots\ldots\ldots\ldots \quad \text{(Equation 5)}$$

Where, TBD = Tapped bulk density, LBD= Loose bulk density.

F. Heckel plot

A single punch machine (KBR Manual Hydraulic Press) equipped with a round flat-faced stainless steel die cavity with a diameter of 10 cm was used for the preparation of the compacts. In advance of the compression, the punch faces and the die wall were lubricated with a 2% magnesium stearate suspension in acetone. Six tablets of 200 ± 3 mg weight were prepared at each of the 6 different compression pressures (0.5, 1, 1.5, 2, 2.5, and 3 tons). Compact weight, hardness, diameter, and thickness of out-of-die tablets, and radius, were measured. Compact density was calculated using its weight (w), diameter (d), and thickness (t). Out-of-die tablet relative density at any compression pressure was calculated as the ratio of compact density to true density. The negative natural logarithm of tablet porosity was taken as its densification. Finally, the graph of ln (1/1-Rd) versus pressure was plotted to analyze the compression properties of the powder compacts [21].

4.3.2 Scanning Electron Microscopy (SEM):

Morphological analysis was performed using Scanning Electron Microscopy (JEOL JSM-6360, Japan). The samples were fixed on a brass stub using double-sided adhesive tape and made electrically conductive by coating in a vacuum (6 Pa) with platinum (6 nm/min) using a Hitachi Ion Sputter (E-1030) for 120 s at 15 mA. The SEM images were analyzed using an image analysis system (ImageInside Ver 2.32) [32].

4.3.3 Particle size determination:

The particle size of all freshly prepared BM-SD formulations was determined by using Zetasizer version 11(Malvern Instruments, Worcestershire, UK) with the manufacturer's software [32].

4.3.4 Drug content determination:

The percentage of drug content in SD was estimated by dissolving the SD equal to 10 mg of BM in 100 mL of methyl alcohol. This solution was further diluted with phosphate buffer (pH 6.8) and the absorbance of each of these solutions was measured at 273 nm [32].

$$\text{Percentage drug content} = \frac{\text{Actual amount of drug}}{\text{Theoretical amount of drug}} 100 \quad \text{(Equation 6)}$$

4.3.5 Saturation solubility studies:

To the glass vials holding 5 mL of phosphate buffer (pH 6.8), each SD was introduced individually. These vials were shaken in the orbital shaker cum incubator at 20 rpm for 24 h at 37±0.5 °C. Samples were filtered using Whatman filter paper (No. 41), and relevant dilutions with phosphate buffer (pH 6.8) were prepared, and finally evaluated spectrophotometrically by detecting absorbance at 273 nm [33]. Depending on the results of drug content and saturation solubility studies, one composition was optimized and used to prepare tablets.

4.4 Formulation of tablet:

The optimized SD (SD5) was passed through # 80 followed by the addition of calculated amounts of each tableting ingredient o form a uniform blend. This blend was gradually supplemented with an appropriate amount of the granulating agent to support tablet formation. The resulting granules were passed through #22/44 and dried at 40 °C for 12 h. On completion of drying, binders HPMC K4M, and MCC were incorporated, followed by the addition of talc as glidant and magnesium stearate as lubricant. The tablets were prepared by the direct compression and evaluated for several pharmacopoeial tests to optimize the formulation [34].

4.5 Evaluation of tablets:

4.5.1 Weight variation:

All 20 tablets from the optimized tablet formulation batch were separately weighed individually. The weight of each tablet was compared against the average weight of

tablets. The following formula was then used to calculate the percent weight variation [35].

$$\%\text{Weight variation} = \frac{\text{Individual weight}}{\text{Average weight}} \times 100 \qquad \text{(Equation 7)}$$

4.5.2 Thickness:

To measure the thickness and diameter, a digital vernier caliper was used. This test was done to examine the uniformity in tablet size and thickness. It was determined by arbitrarily picking 5 tablets from each formulation and measuring with a vernier caliper to calculate the mean thickness [35].

4.5.3 Hardness:

The hardness of the tablet depends on the quantity of material filled in the die and the amount of compressional force applied. Tablet hardness affects the resistance offered by them during handling, transportation, or storage before use. Tablets' hardness was determined by employing a Monsanto hardness tester [36]. The top plunger was pushed against a spring by spinning the threaded bolt while the lower plunger was kept in contact with the tablet, and the reading recorded was zero. A hardness test for tablets was conducted on randomly selected 5 tablets from the optimized batch. This force applied continued until the tablet broke. The fracture force was measured and subtracted from the zero-force value [37].

4.5.4 Friability:

The Veego friabilator was used to test friability. Normally, a pre-weighed tablet sample from each created batch was placed in a friabilator and rotated 100 times. After a subsequent reweigh, the tablets were measured again, and the following formula was used to determine the % loss [35].

$$\%\text{Friability} = \frac{\text{Initial weight} - \text{Final weight}}{\text{Initial weight}} \times 100 \qquad \text{(Equation 8)}$$

4.5.5 *In vitro* disintegration time:

The USP disintegration tester was used to conduct a disintegration test, (Model ED-2L, Electrolab, Mumbai). In order to perform this test, the disintegration medium used was phosphate buffer (pH 6.8) kept at 37 ±2 °C. A total of 6 tablets were put in the tubes of a tester, and the amount of time it took for each tablet to disintegrate and dissolve in the medium without leaving any residue was noted [37].

4.5.6 Drug content:

The weight of randomly selected 5 tablets was recorded individually and the average weight was calculated. These tablets were powdered in a mortar using a pestle. The powder weight equivalent to 40 mg of BM was transferred into a volumetric flask containing phosphate buffer (pH 6.8) and the volume was made up to 100 mL. Further, the solution was kept aside for a day to allow for the complete dissolution of the drug. This solution was then diluted to obtain a solution of strength 10 µg/mL. This diluted solution was filtered, and absorbance was recorded at 273 nm on a UV-visible spectrophotometer [36].

4.5.7 XRPD Analysis:

XRPD analysis of powdered samples was accomplished by using an X-ray diffractometer (Bruker, Germany). It was used to measure the angle of diffraction in the range of 4 - 40º within the reproducibility limit of ±0.001. The rate meter's scanning speed of 2ºθ/min was used to record the XRPD pattern automatically. The XRPD patterns of pure drug and formulation were recorded and analyzed [38].

4.5.8 FTIR Analysis:

A Diffuse Reflectance Fourier Transform Infrared Spectroscopy (DRS-FTIR) (Bruker, Germany) was used to obtain the FTIR spectra of BM and tablet formulation. Dry KBr was mixed with 2 to 3 mg of samples, and the spectra were scanned throughout a wave number in the range of 4000 to 400 cm^{-1} [39].

4.5.9 DSC Analysis:

The DSC thermogram of the BM and its tablet formulation was used obtained using Hitachi 7020 to assess its thermal behavior. The sample was heated at a

constant rate of 10 °C/min throughout a temperature range of 25 - 350 °C while being hermetically enclosed in aluminum pans. An inert atmosphere was maintained by purging with nitrogen at a flow rate of 60 mL/min [40].

4.5.10 Dissolution study:

In vitro drug release studies provide information about the amount of drug released from the formulation. The dissolution of the tablets was examined using USP XXII type II dissolution test equipment (Electrolab-TDT 08L). These paddles are placed in a vessel containing the dissolution medium in the dissolution test apparatus, rotating at 50 r.p.m. Aliquots were taken out at scheduled time intervals of up to 9 hrs and evaluated spectrophotometrically using a UV-visible spectrophotometer (Jasco V630) at a maximum wavelength of 273 nm [35].

4.5.11 Drug release kinetics study:

The drug release profile of the optimized SD was examined to calculate R2 and to verify the type of model it follows. Models tested include zero-order, first-order, Higuchi models, and Korsmeyer and Peppas model [41].

4.5.12 Stability Study:

Investigation of physical changes in an optimized tablet formulation was performed by short-term stability studies such as drug content and drug release. As a formal prerequisite for the licensing of pharmaceuticals for human consumption, the FDA and ICH define standards for stability testing of new medicinal products. To conduct stability tests on promising formulations, tablets were kept at a temperature of 40 °C and relative humidity (75%) for three months [42,43].

REFERENCES

1. Tran P, Pyo YC, Kim DH, Lee SE, Kim JK, Park JS. Overview of the manufacturing methods of solid dispersion technology for improving the solubility of poorly water-soluble drugs and application to anticancer drugs. *Pharmaceutics*. 2019 Mar 19; 11(3):132.
2. Sareen S, Joseph L, Mathew G. Improvement in solubility of poor water-soluble drugs by solid dispersion. *International Journal of Pharmaceutical Investigation*. 2012; 2(1):12.
3. Bhalani DV, Nutan B, Kumar A, Singh Chandel AK. Bioavailability Enhancement Techniques for Poorly Aqueous Soluble Drugs and Therapeutics. *Biomedicines*. 2022 Aug 23; 10(9):2055.
4. Attia MS, Hasan AA, Ghazy FE, Gomaa E, Attia M. Solid dispersion as a technical solution to boost the dissolution rate and bioavailability of poorly water-soluble drugs. *Indian Journal of Pharmaceutical Education and Research*. 2021 Apr 1; 55(13):103.
5. Pawar SR, Barhate SD. Solubility enhancement (Solid Dispersions) novel boon to increase bioavailability. *Journal of Drug Delivery and Therapeutics*. 2019 Mar 22; 9(2):583-90.
6. Alanazi FK, El-Badry M, Ahmed MO, Alsarra IA. Improvement of albendazole dissolution by preparing microparticles using spray-drying technique. *Scientia Pharmaceutica*. 2007 Jun; 75(2):63-80.
7. Manogna K, Nagaveni P, Thyagaraju K. Enhancement of solubility of poorly soluble drugs by solid dispersion: An overview. *Indian Journal of Pharmaceutical and Biological Research*. 2017 Dec 31; 5(04):17-23.
8. Ha ES, Baek IH, Cho W, Hwang SJ, Kim MS. Preparation and evaluation of solid dispersion of atorvastatin calcium with Soluplus® by spray drying technique. *Chemical and Pharmaceutical Bulletin*. 2014 Jun 1; 62(6):545-51.
9. Dangre PV, Sormare VB, Godbole MD. Improvement in dissolution of bosentan monohydrate by solid dispersions using spray drying technique. *Open Pharmaceutical Sciences Journal*. 2017 Apr 28; 4(1).

10. Nagarsenker MS, Meshram RN, Ramprakash G. Solid dispersion of hydroxypropyl β- cyclodextrin and ketorolac: enhancement of *in vitro* dissolution rates, improvement in anti- inflammatory activity and reduction in ulcerogenicity in rats. *Journal of pharmacy and pharmacology*. 2000 Aug; 52(8):949-56.
11. Tekade AR, Yadav JN. A review on solid dispersion and carriers used therein for solubility enhancement of poorly water-soluble drugs. *Advanced pharmaceutical bulletin*. 2020 Jul; 10(3):359.
12. Gallardo D, Skalsky B, Kleinebudde P. Controlled release solid dosage forms using combinations of (meth) acrylate copolymers. *Pharmaceutical development and technology*. 2008 Jan 1; 13(5):413-23.
13. Kindermann C, Matthée K, Strohmeyer J, Sievert F, Breitkreutz J. Tailor-made release triggering from hot-melt extruded complexes of basic polyelectrolyte and poorly water-soluble drugs. *European journal of pharmaceutics and biopharmaceutics*. 2011 Oct 1; 79(2):372-81.
14. Drašković M, Medarević D, Aleksić I, Parojčić J. *In vitro* and *in vivo* investigation of taste-masking effectiveness of Eudragit E PO as drug particle coating agent in orally disintegrating tablets. *Drug development and industrial pharmacy*. 2017 May 4; 43(5):723-31.
15. Dingemanse J, van Giersbergen PL. Clinical pharmacology of bosentan, a dual endothelin receptor antagonist. *Clinical pharmacokinetics*. 2004 Dec; 43:1089-115.
16. Moradi M, Rahimpour E, Jafari P, Jouyban A. Solubility Measurement and Mathematical Modeling for Bosentan in Mixtures of Ethylene Glycol and Water at 293.15–313.15 K. *Journal of Solution Chemistry*. 2023 Feb; 52(2):218-27.
17. Saffoon N, Uddin R, Huda NH, Sutradhar KB. Enhancement of oral bioavailability and solid dispersion: a review. *Journal of Applied Pharmaceutical Science*. 2011 Sep 30(Issue):13-20.
18. Sharma A, Jain CP. Solid dispersion: A promising technique to enhance solubility of poorly water-soluble drug. *International Journal of Drug Delivery*. 2011 Apr 1; 3(2):149.
19. Kumar B. Solid dispersion-a review. *PharmaTutor*. 2017 Feb 1; 5(2):24-9.
20. Khachane P, Nagarsenker MS. Eudragit EPO nanoparticles: application in improving therapeutic efficacy and reducing ulcerogenicity of meloxicam on oral administration. *Journal of biomedical nanotechnology*. 2011 Aug 1; 7(4):590-7.
21. Yadav PS, Hajare AA, Patil KS. Development of Doxazosin mesylate liquisolid system for improved manufacturing processability and bioavailability: in vitro and in vivo evaluation for tailored hypertension treatment approach with modified dissolution rates. *Journal of Dispersion Science and Technology*. 2023 Apr 18:1-4.
22. Kzar HH, Al-Gazally ME, Wtwt MA. Everolimus loaded NPs with FOL targeting: preparation, characterization and study of its cytotoxicity action on MCF-7 breast cancer cell lines. *Jordan Journal of Pharmaceutical Sciences*. 2022 Mar 1; 15(1):25-39.
23. Kraisit PA. Impact of hydroxypropyl methylcellulose (HPMC) type and concentration on the swelling and release properties of propranolol hydrochloride matrix tablets using a simplex centroid design. *Int. J. Appl. Pharm*. 2019; 11:143-51.
24. Thoorens G, Krier F, Leclercq B, Carlin B, Evrard B. Microcrystalline cellulose, a direct compression binder in a quality by design environment—A review. *International journal of pharmaceutics*. 2014 Oct 1; 473(1-2):64-72.
25. Jadhav NR, Paradkar AR, Salunkhe NH, Karade RS, Mane GG. Talc: A versatile pharmaceutical excipient. *World Journal of Pharmacy and Pharmacutical Sciences*. 2013 Aug 22; 2:4639-60.
26. Morin G, Briens L. The effect of lubricants on powder flowability for pharmaceutical application. *AAPS Pharmscitech*. 2013 Sep; 14(3):1158-68.
27. Comoglu T, Dilek Ozyilmaz E. Orally disintegrating tablets and orally disintegrating mini tablets–novel dosage forms for pediatric use. *Pharmaceutical Development and technology*. 2019 Aug 9; 24(7):902-14.

28. Patil KS, Hajare AA, Manjappa AS, More HN, Disouza JI. Design, development, *in silico* and *in vitro* characterization of Docetaxel-loaded TPGS/ Pluronic F 108 mixed micelles for improved cancer treatment. *Journal of Drug Delivery Science and Technology*. 2021 Oct 1; 65.
29. Hajare AA, Velapure PD, Rathod PN, Patil KS, Chopade SS. Formulation and evaluation of solid lipid nanoparticle gel for topical delivery of clobetasol propionate to enhance its permeation using silk sericin as permeation enhancer. *International Journal of Pharmaceutical Sciences and Research* [Internet]. 2020; 11(5).
30. Xu H, Liu L, Li X, Ma J, Liu R, Wang S. Extended tacrolimus release via the combination of lipid-based solid dispersion and HPMC hydrogel matrix tablets. *Asian Journal of Pharmaceutical Sciences*. 2019 Jul 1; 14(4):445-54.
31. Ala'Y S, AlRashdan Y, Abbasi NU, Mostafa A, Abudayeh Z, Talhouni A, Al-Ebini Y. Optimization and Validation of HPLC-UV Method for the Determination of Vardenafil, Sildenafil, and Tadalafil in Honey-Mixed Herbal Sachets Using a Design of Experiment. *Jordan Journal of Pharmaceutical Sciences*. 2023 Mar 25; 16(1):148-62.
32. Khanfar M, Salem MS. Dissolution enhancement of poorly water-soluble drugs by co-precipitation in the presence of additives and stabilizers. *Jordan journal of pharmaceutical sciences*. 2009; 2(1).
33. Nandi U, Ajiboye AL, Patel P, Douroumis D, Trivedi V. Preparation of solid dispersions of simvastatin and soluplus using a single-step organic solvent-free supercritical fluid process for the drug solubility and dissolution rate enhancement. *Pharmaceuticals*. 2021 Aug 25; 14(9):846.
34. Mittal A, Yadav M, Choudhary D, Shrivastava B. Enhancement of solubility of lurasidone HCl using solid dispersion technique. *International Journal of Research in Ayurveda & Pharmacy*. 2014 Nov 27; 5(5):632–7.
35. Das A, Nayak AK, Mohanty B, Panda S. Solubility and Dissolution Enhancement of Etoricoxib by Solid Dispersion Technique Using Sugar Carriers. ISRN *Pharmaceutics*. 2011 Sep 5; 2011:1–8.
36. Chandana CH, Kumar YG, Vishnu YV, Madhuri MM. Metoprolol succinate sustained release matrix tablets-formulation development and *in vitro* evaluation.
37. Bookya P, Raparla R, Sriramula HP, Tarrigopula S, Vanga S. Formulation and evaluation of metformin hydrochloride sustained-release oral matrix tablets. *Asian Journal of Pharmaceutical and Clinical Research*. 2018 Mar 1; 11(3):342–5.
38. Patil SS, Chougale RD, Manjappa AS, Disouza JI, Hajare AA, Patil KS. Statistically developed docetaxel-laden mixed micelles for improved therapy of breast cancer. *OpenNano*. 2022 Nov 1; 8:100079.
39. Hajare A, Dol H, Patil K. Design and development of terbinafine hydrochloride ethosomal gel for enhancement of transdermal delivery: In vitro, in vivo, molecular docking, and stability study. *Journal of Drug Delivery Science and Technology*. 2021 Feb 1; 61:102280.
40. Kerdsakundee N, Mahattanadul S, Wiwattanapatapee R. Development and evaluation of gastroretentive raft forming systems incorporating curcumin-Eudragit® EPO solid dispersions for gastric ulcer treatment. *European Journal of Pharmaceutics and Biopharmaceutics*. 2015 Jul 18; 94:513–20.
41. Patil K, Patil J, Bharade S, Disouza J, Hajare A. Design and development of sodium alginate/carboxymethyl cellulose in situ gelling system for gastroretentive delivery of lisinopril. *Journal of Research in Pharmacy*. 2023 Mar 1; 27(2).
42. Altamimi MA, Neau SH. Investigation of the *in vitro* performance difference of drug-Soluplus® and drug-PEG 6000 dispersions when prepared using spray drying or lyophilization. *Saudi Pharmaceutical Journal*. 2017 Mar 1; 25(3):419–39.

43. Patil PB, Hajare AA, Awale RP. Development and Evaluation of Mesalamine Tablet Formulation for Colon Delivery. *Research Journal of Pharmacy and Technology*. 2011 Nov 28; 4(11):1751-6.
44. Reynolds R., Potz N., Colman M., Williams A., Livermore D. and MacGowan A. BSAC Extended Working Party on Bacteremia Resistance Surveillance. Antimicrobial sensitivity of the pathogens of bacteremia in the UK and Ireland 2001-2: the BSAC Bacteremia Resistance Surveillance Programme. *J. Antimicrob. Chemother*. 2004; 53:1018—1032.
45. Ochocinski D., Dalal M., Black V. L., Carr S., Lew J., Sullivan K. and Kissoon N. Life threatening Infectious Complications in Sickle cell Disease: A concise Narrative Review. *Front Pediatr.* 2020; 8(38): 1-22
46. Roskov Y., Ower G., Orrell T., Nicolson D., Bailly N., Kirk P. M., Bourgoin T., Dewalt R. E., Decock W., Nieukerken E. and Penev L. Specie 2000. *Naturalis, Leiden, the Netherland*, 2020.
47. Global Biodiversity Information Facility Secretariat. Ficus thonningii Blume. GBIF Backbone Taxonomy. Checklist dataset, 2019. [online]. Available: https://hosted-datasets.gbif.org/datasets/backbone/
48. Harborne J. B. Phytochemical Methods- A guide to modern Techniques of plant analysis. 3rd edition, Chapman and Hall, London, 1988, pp.1-230.
49. Adeniyi B. A., Odelola H. A. and Oso B. A. Antimicrobial potential of *Diospyros mesiliforus* (*Ebenaceae*). *Afr. J. Med. Med Sci*. 1996; 25(3):221-224.
50. Cheesbrough M. Antimicrobial susceptibility testing. District Laboratory Practice in tropical countries part 2, 2nd edition, Cambridge University press, United Kingdom, 2000, pp. 132-143.
51. Esimone C. O., Adikwu M. U. and Okonta J. M. Preliminary antimicrobial screening of ethanolic extract from the lichen *Usnea subfloridans* (L). *J. Pharm. Res. Dev.* 1998; 3(2): 99-101.
52. Adebayo E. A., Ishola O. R., Taiwo O. S., Majolagbe O. N. and Adekeye B. T. Evaluations of the methanol extract of *Ficus exasperata* stem bark, leaf and root for phytochemical analysis and antimicrobial activities. *Afr. J. Plant Sci.* 2009; 3(12): 283-287.
53. Chavan M. C., Navratne A. R., Patil R. B., Vanjari S. S. and Khandelwal K. R. Development and validation of stability indicating high performance thin layer chromatography method for analysis of Bergapten. *J. Pharm. Sci. Res.* 2019; 11(9):3237-3242.
54. Chunyan C., Bo S., Ping L., Jingmei L. and Ito Y. Isolation and purification of psoralen and bergapten from *Ficus carica* l leaves by high-speed countercurrent chromatography. *J. Liq. Chromatogr. Relat. Technol.* 2009; 32(1):136–143
55. Liu R., Feng L., Sun A. and Kong L. Preparative isolation and purification of coumarins from *Cnidium monnieri* (L.) Cusson by high-speed counter-current chromatography. *J. Chromatogr. A*. 2004; 20014(1005): 71–76.
56. Sahil K. and Souravh B. A. Review of protocatechuic acid and its pharmacological potential. *Int. Sch. Res. Notices.* 2014; 12(952943).
57. Benahmed M., Akkal S., Elomri A., Laouer H., Verite P. and Seguin E. Constituents from *Bulpleurum montanum* (Coss and Dur) (*Apiaceae*). *Arabian J. Chem.* 2011; 1-5.
58. Ijoma K. I. and Ajiwe V. I. E. Methyl ferulate induced conformational changes on DeOxyHbS: Implication on sickle erythrocyte polymerization. *Mediterr. J. Chem.* 2022; 12(1):100-111
59. Madeiro A. L., Borges H. P. B., Souto A. L., Figueiredo T. R., Siqueira-Junior J. P. and Tavares J. F. Modulation of the antibiotic activity against multidrug resistant strains of coumarins isolated from Rutaceae species. *Microb. pathog.* 2017; 104:151-154

60. Quetglas-Llabres M. M., Quipe C., Herrera-Bravo J., Catarino M. D., Pereira O. R., Cardoso S. M., Dua K., Chellappan D. K., Pabreja K., Satija S., Mehta M., Sureda A., Martorell M., Satmbekova D., Yeskaliyeva B., Sharifi-Rad J., Rasool N., Butnariu M., Bagiu C. J, Bagiu R. V, Calina D. and Cho W. C. Pharmacological properties of bergapten: mechanistic and therapeutic aspects. *Oxid. Med. Cell. Longev*. 2022; 8615242: 1-10.
61. Semaming Y., Pannengpetch P., Chattipakorn S. C. and Chattipakorn N. Pharmacological properties of protocatechuic acid and its potential roles as complementary medicine. *Evid-Based. Complement. Altern. Med*. 2015; 593902: 1-11.
62. Li T., Shen Y., Chen H., Xu Y., Wang D., Cui F., Han Y. and Li J. Antimicrobial properties of coaxial spinning membrane of methyl ferulate/zein and its preservation effects on Sea Bass. *Foods*. 2021; 10(10): 2385, 1-15.
63. Wang W., Sun Q., Gan N., Zhai Y., Xiang H. and Li H. Characterizing the interaction between methyl Ferulate and human serum albumin by saturation transfer difference NMR. *RSC. Adv.* 2020; 10(54): 32999-33009.
64. Ijoma K. I. and Ajiwe V. I. E. *Jatropha tanjorensis* a flora of Southeast Nigeria: Isolation and Characterization of naringenin and validation of bio-enhanced synergistical activity of α-tocopherol toward clinical isolates of resistant bacterial. *Makara J. Sci.* 2022; 26(2): 120-127
65. Dangarembizi R., Erlwanger K. H., Moyo D. and Chivandi E. Phytochemistry, Pharmacology and Ethnomedicinal uses of Ficus thonningii (blume moraceae): A Review. *Afr. J. Tradit. Complement. Altern. Med*. 2013; 10(2): 203-212
66. Cousins O. N. and Michael A. H. Medicinal properties in the diet of Gorillas. An ethno-pharmacological evaluation, *Afr. Study Monogr*. 2002; 23(2): 65-89
67. Barret-Connor E. Bacterial infection and sickle cell anaemia. *Medicine (Baltimore)*. 1971; 50(2): 97-112.
68. Powars D., Overturf G. and Turner E. Is there an increased risk of Haemophilus influenzae septicemia in children with sickle cell anemia? *Pediatr.* 1983; 71(6): 927–931
69. Wright J., Thomas P. and Serjeant G. R. Septicemia caused by salmonella infection: an overlooked complication of sickle cell disease. *J. Pediatr.* 1997; 130(3): 394–399.
70. Amyes S. Antimicrobial chemotherapy: Pocketbook. Chemical Rubber Company Press, Florida, USA, 1996, p25.
71. French G. L. Bactericidal agents in the treatment of MRSA infections-the potential role of daptomycin. *J. Antimicrob. Chemother*. 2006; 58(6): 1107-1117
72. Alima Yanda A. N, Nansseu J. R., Awa H. D., Tatah S. A., Seungue J., Eposse C. and Koki P. O. Burden and spectrum of bacterial infections among sickle cell disease children living in Cameroon. *BMC. Infect. Dis.* 2017; 17(21): 1-7.
73. Sowndhariya, S., Ravi, S., Dharani, J. and Sripathi, R. Chemical constitution, in silico molecular docking studies and antibacterial activity of flower essential oil of Artabotrys hexapetalus. *Jordan J. Pharm. Sci.* 2022; 15(3):341-354.
74. Mbang, N.F., Olutayo, A.A., Lateef, G.B., Oluyemisi, A.B., Florence, O.O., Olufunke, C.B. and Khalidat, O.O. Evaluation of the antimicrobial activity of *Strombosia grandifolia* Hook f.ex Benth extract hand sanitizer formulation. *Jordan J. Pharm. Sci.* 16(1):61-71.

تكوين وتطوير وتقييم أقراص تشتت صلبة بالتجفيف بالرش لبوسنتان مونوهيدرات لتحسين ملف الذوبانية

سيالي راوت[1]، أشوك هاجر [*] [2]، روتوجا شوجال[3]، شوبهام كامبل[1]، كيران باتيل[3]

[1] قسم الصيدلانيات، كلية بهاراتي فيديابيث للصيدلة، بالقرب من تشيتراناغاري، كولهابور، ماهاراشترا، الهند .

[2] قسم التكنولوجيا الصيدلانية، كلية بهاراتي فيديابيث للصيدلة، بالقرب من تشيتراناغاري، كولهابور، ماهاراشترا، الهند.

[3] قسم ضمان جودة المستحضرات الصيدلانية، كلية الصيدلة تاتياساحب كور، واراناجار، ماهاراشترا، الهند.

ملخص

بوسنتان مونوهيدرات (BM) يستخدم لعلاج ضغط الشرايين الرئوية. لديه قابلية ضعيفة للذوبان في الماء وانتشارية حيوية منخفضة. تهدف الدراسة الحالية إلى تحسين معدل الذوبان للأدوية باستخدام إيودراجيت® إي بي أو عن طريق التجفيف بالرش. تم استخدام الدواء وإيودراجيت® إي بي أو بنسبة 1:1، 1:2، 1:3، 1:4، و 1:5 (وزن/وزن) لإنتاج التراكيب SD1 إلى .SD5 أظهر SD5 بنسبة الدواء إلى الحامل 1:5 زيادة ملحوظة إحصائيًا في ذوبانية التشبع ومحتوى الدواء. تم إنشاء 6 تركيبات للأقراص تحتوي على SD5 ومكونات التحبيب، مرقمة من F1 إلى F6 وتم معالجتها. لوحظت أعلى معدل ذوبان وإطلاق للدواء في التركيبة F2 التي تحتوي على HPMC K4M 26.36% و MCC. 23.63% الآلية المحتملة المعنية بذوبان BM في SD هي شكله البلوري والتأثير المحلل للدواء الذي يتمثل في التآزر بين BM وإيودراجيت® إي بي أو. قد يكون قوة الشد العالية وقلة التلف ووقت الانحلال الطويل نتيجة لتأثير الربط المظهري للحامل. قد تكون الخلط المباشر لـ SD مع HPMC قد ساهم في تحسين التجانس لـ SD داخل مصفوفة الأقراص وملف الإفراج. هذه الدراسة أوضحت ملائمة التجفيف بالرش في تحضير SD من BM مع إيودراجيت® إي بي أو، مما يمكن أن يحسن قابلية الذوبان والاستقرار للدواء.

الكلمات الدالة: بوسنتان مونوهيدرات، إيودراجيت® إي بي أو، قابلية الذوبان، الذوبان، التشتت الصلب، التجفيف بالرش.

[*] ***المؤلف المراسل: أشوك هاجر***

i ashok.hajare@bharatividyapeeth.edu

تاريخ استلام البحث: 2022/10/6 وتاريخ قبوله للنشر: 2023/6/25.